

*EVS28*  
*KINTEX, Korea, May 3-6, 2015*

## **DC-Electric Vehicle Supply Equipment Operation Strategies for Enhanced Utility Grid Voltage Stability**

Peter Krasselt<sup>1</sup>, Jonas Boßle, Michael R. Suriyah, Thomas Leibfried

<sup>1</sup>*Karlsruhe Institute of Technology, Institute of Electric Energy Systems and High-Voltage Technology, Engesserstr. 11, 76133 Karlsruhe, Germany, peter.krasselt@kit.edu*

---

### **Abstract**

High-power DC electric vehicle supply equipments (EVSE) have a significant impact on voltage stability in low-voltage networks. To ensure the guaranteed voltage characteristics, utility grid operator permit the installation of DC-EVSE only in proximity of local substations. A simplified grid access strategy for DC-EVSE is achievable by reactive power support of the EVSE rectifier system. Since decentralized regenerative energy (DRE) already provide voltage band control using reactive power support in low-voltage networks, the interaction of DRE and EVSE reactive power compensation scheme is investigated. To enhance power converters operation, a fast reacting voltage-droop control concept for DRE and EVSE is proposed for rapid voltage change mitigation. The applicability of a voltage-droop control is verified using probabilistic simulations.

*Keywords: fast-charging, electric vehicle supply equipment, reactive voltage support, voltage-droop control*

---

## **1 Introduction**

### **1.1 Public Electric Vehicle Fast Charging Infrastructure**

The majority of Electric Vehicle (EV) trips can be covered by normal power recharging offering an AC connection power from 3,7 kW up to 22 kW. However, to fulfill the requirements of long distance trips and flexible spontaneous route planning, a fast charging infrastructure is necessary. For 2020, a demand for a public charging infrastructure consisting of 173.000 normal power recharging points (22 kW, AC charging) und 7.100 high power recharging points (50 kW, DC charging) is predicted in Germany [1]. Connecting fast-charging DC electric vehicle supply equipment (EVSE) to a low-voltage (LV) network has a significant impact on power quality.

### **1.2 Standards and Technical Rules for EVSE Network Connection**

To ensure the standardized voltage characteristics in public distribution networks [2], several standards and technical rules have to be met for grid access of an EVSE in Germany. As demanded in [3], the EVSE operator requests a network connection for a load exceeding 12 kW rated power from the distribution network operator. As the common range of standardization for loads connected to low-voltage networks is limited to currents up to 75 A [4,5], an individual technical assessment of network disturbance [6] has to be done.

## 2 Assessment of Network Disturbance for Typical EVSE

For the assessment of network disturbance, the following aspects are considered:

- First, the characteristics of EVSE with passive and active front-end rectifiers are summarized.
- Next, typical LV network characteristics are analyzed, as the network disturbance has to be calculated at the point of common coupling (PCC).
- This is followed by a discussion of the most relevant disturbance types.

### 2.1 EVSE Operation Characteristics

The total efficiency  $\eta$  of a DC-EVSE, measured from the AC power consumption to the DC charging power, can be estimated as 95 %. With a DC charging power of 50 kW, the rated AC power is 53 kVA, resulting in an AC three phase power connection request of at least 3x80 A.

The key component for the impact on power quality in LV-networks is the rectifier topology. Most EVSE interface AC mains with a passive line-commutated rectifier as shown in Figure 1a.

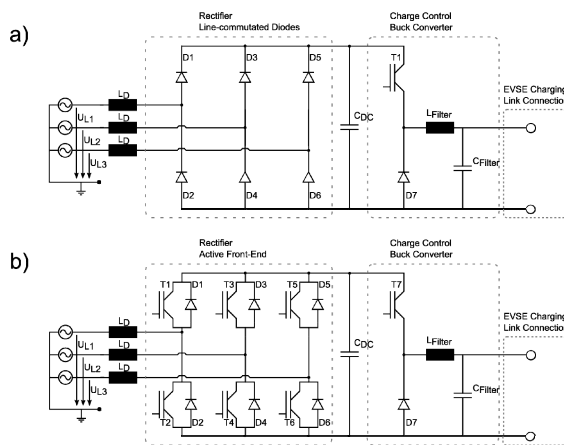


Figure 1: Considered EVSE-Topologies

- a) standard line-commutated rectifier
- b) proposed self-controlled rectifier

This rectifier type draws an inductive power factor  $\lambda$  of 0,96 at rated power operation. The total harmonic distortion of the line currents (THD<sub>I</sub>) is limited by technical measures (AC commutating reactor and DC smoothing reactance) in the range of 40 to 70 %.

The EVSE in Figure 1b is equipped with an active front-end. Using IGBTs, this self-

commutated rectifier draws a nearly sinusoidal current with a THD<sub>I</sub> lower than 10 %. This rectifier topology also features full independent control of the reactive power consumption.

### 2.2 Network Characteristics

A key factor for the assessment of network disturbances is the grid impedance at the PCC of the EVSE. The impedance at a PCC can be calculated by using the network diagram shown in figure 2. As it is more convenient for calculations, the grid impedance is usually expressed in the short-circuit power  $S_{SC,PCC}$  and the network impedance ratio  $R/X$ .

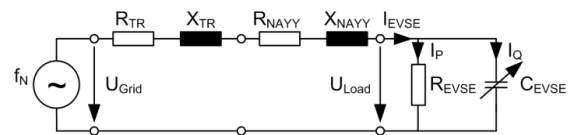


Figure 2: Single-Line Network diagram of LV-network

The high-voltage and medium voltage network are modelled in the source resistance  $R_S$  and impedance  $L_S$ . A standard local substation 20kV/0,4kV transformer with a rated power of 400 kVA feeds a LV cable type NAYY4x150mm<sup>2</sup>, which is the most used standard cable in German LV networks [7]. With the parameters given in table 1, the short-circuit power and R/X ratio is calculated for variable cable length (figure 3).

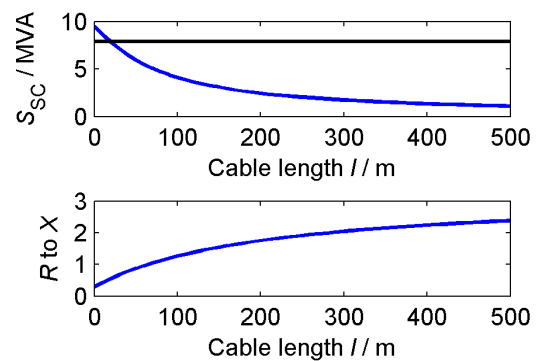


Figure 3:

- Upper plot: Short-circuit power (blue), required short-circuit power for uncontrolled rectifier (black).
- Lower plot: R/X ratio for variable LV cable length

Table 1: Network parameters used in Figure 2

Parameter	Value	Unit	Description
$U_{\text{Grid}}$	400	V	Nominal voltage
$f_{\text{N}}$	50	Hz	Power frequency
$R_{\text{TR}}$	5,7	m $\Omega$	Transformer resistance
$L_{\text{TR}}$	70	$\mu\text{H}$	Transformer inductance
$R'_{\text{NAYY}}$	256	m $\Omega/\text{km}$	Resistance per unit length
$L'_{\text{NAYY}}$	255	$\mu\text{H}/\text{km}$	Impedance per unit length
$R_{\text{S}}$	620	$\mu\Omega$	Source resistance
$L_{\text{S}}$	2,6	$\mu\text{H}$	Source inductance

## 2.3 Assessment of Network Disturbance for EVSE

### 2.3.1 Harmonic Voltages

EVSE rectifiers inject harmonics in the power system. Due to the line impedance, harmonic voltages build up.

In case of an EVSE with a 6-pulse *line-commutated rectifier* (figure 1 a), a short-circuit power 150 times higher [6] than EVSE rated power (shown as black curve in figure 3) is required for grid access. The critical line length providing this amount of short-circuit power is 20 m. For longer cable distances, additional measures have to be taken for harmonic current limitation, e.g. use of a 12-pulse rectifier fed by a three-winding transformer.

An EVSE featuring a *self-commutated rectifier* meets harmonic emission requirements with ease. With a  $\text{THD}_I$  smaller than 10 %, no harmonic assessment has to be done. To suppress interharmonic voltage emission, the IGBT switching frequency has to be locked to an integer ratio synchronous to the grid frequency.

### 2.3.2 Rapid Voltage Changes

Fast fluctuations in electrical power consumption generate rapid voltage changes. While starting a charging process, EVSE avoid flicker emission with a slow power-on ramp over several seconds. During charging and towards the end of the charging process, power fluctuation are small, so

rapid voltage changes are no limiting factor for the installation of EVSE.

### 2.3.3 Supply Voltage Variations

The charging time of an EV is estimated to be at least 10 min. Therefore, the change rate  $r$  for supply voltage variation is  $r = 0,1 \text{ min}^{-1}$  and the maximum tolerated voltage drop  $d_{\text{max,LV}}$  due to charging activity is 3 % of nominal network voltage  $U_{\text{Grid}}$  [6]. This crucial criterion defines the maximal line length between a local substation and an EVSE and is investigated in detail in this study.

## 2.4 Proposed EVSE Topology

Offering the feature of independent regulated reactive power and low harmonic voltage emission, an EVSE with a self-commutated active front-end is selected. The active-rectifier is dimensioned for a power factor of 0.9 at rated power, resulting in a total connection power of 60 kVA fed by a three phase AC connection 3x100 A.

## 3 Reactive Power Support for Grid Integration in LV-Networks

### 3.1 Expansion of Maximal Line Length by Reactive Power Support

#### 3.1.1 Analytical Approach

First, the principle effect on supply voltage variations during EVSE operation and the reactive power support to reduce voltage drop is analytically investigated. The voltage amplitude drop  $U_{\Delta}$  during EVSE operation at the EVSE PCC is expressed in equation 1 by applying the Kapp triangle shown in Figure 4.

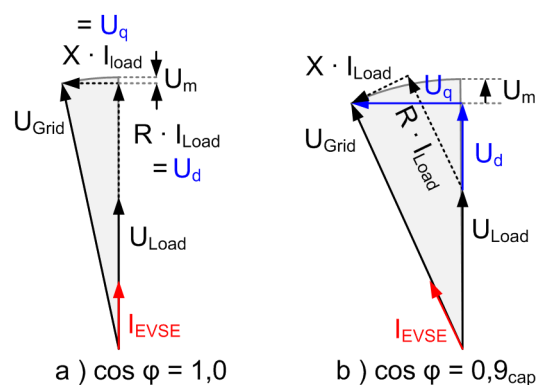


Figure 4: Kapp triangle for a) unity and b) capacitive-ohmic power factor.

$$U_{\Delta} = U_{Grid} - U_{Load} = U_d + U_m \quad (1)$$

$$U_d = R \cdot I \cdot \cos \varphi + X \cdot I \cdot \sin \varphi \quad (2)$$

$$U_q = X \cdot I \cdot \cos \varphi + R \cdot I \cdot \sin \varphi \quad (3)$$

Using the example LV network shown in figure 2, the resistance  $R$  and inductance  $X$  is given by

$$\begin{aligned} X &= X_S + X_{TR} + X_{NAYY}, & X_{NAYY} &= X'_{NAYY} \cdot l \\ R &= R_S + R_{TR} + R_{NAYY}, & R_{NAYY} &= R'_{NAYY} \cdot l \end{aligned} \quad (4)$$

where  $l$  is the cable line length. The current  $I$  is calculated from the EVSE active power drawn from the AC mains. The EVSE power factor is calculated by

$$\begin{aligned} I &= \sqrt{I_P^2 + I_Q^2} \\ I_Q &= I_P \cdot \tan(\cos^{-1} \varphi) \end{aligned} \quad (5)$$

Using the geometric relations defined in Figure 4,  $U_m$  can be defined by the following equation:

$$(U_{Grid} - U_m)^2 + U_q^2 = U_{Grid}^2 \quad (6)$$

By substituting  $U_m$  in (1) using (6), the voltage amplitude drop between  $U_{Grid}$  and  $U_{EVSE}$  is now defined by

$$U_{\Delta} = U_d + U_{Grid} - \sqrt{U_{Grid}^2 - U_q^2} \quad (7)$$

### 3.1.2 Calculation of Maximal Line Length

The maximal cable length between the local substation and the PCC can be calculated by solving equation (1) for

$$U_{\Delta} = d_{\max} = 3\% \cdot U_{Grid}, \quad (8)$$

calculating with the rated current value and unity power factor in (2),(3) and (5):

$$I_P = 80 \text{ A} \quad \text{and} \quad \varphi = 0^\circ. \quad (9)$$

As we can see in the upper plot of figure 5, the maximal line length is determined as 330 m. For longer distances, a capacitive power factor has to be increased to preserve the  $d_{\max}$  criterium. With respect to the minimal required power factor of 0.9 [3] for LV connected loads, the maximum line length can be increased by 30 % to 429 m (lower plot in figure 5).

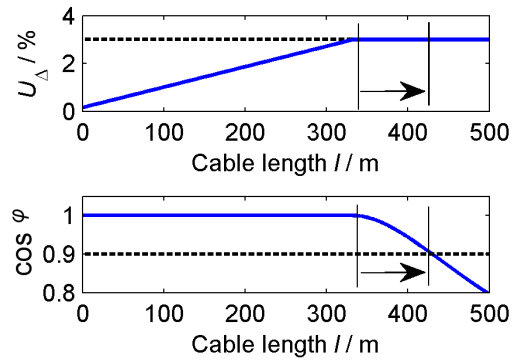


Figure 5:

Upper plot: Voltage drop for variable cable length  $l$   
Lower plot: Required  $\cos \varphi_{EVSE}$  to ensure  $d_{\max} = 3\%$

The benefit of simplified grid access by reactive power support of EVSE comes at the cost of increased grid and inverter losses. With increasing reactive power consumption, the EVSE draws an increasing line current  $I_{EVSE}$  (figure 6).

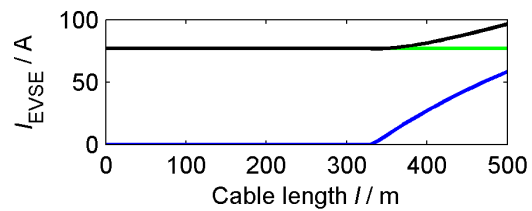


Figure 6: EVSE currents  $I_{EVSE}$ , Rated current (black), active current  $I_P$  (green) Reactive current  $I_Q$  (blue)

With the increasing number of power converters for DRE generation and the integration of new load type like EVSE, the reactive power control scheme has to be chosen with special care. Therefore, the efficiency of different approaches is discussed in the following chapter.

## 3.2 Voltage Support Control Concepts

### 3.2.1 Power Factor Based Concepts

Reactive power support is already used in LV-networks. As voltage amplitude rises due to DRE infeed, the DRE inverters provide inductive reactive power to ensure LV-network voltage stability. It is common practice [8] to use the reactive power control schemes as shown in table 2. Inspired by these control schemes, three possible implementations are adapted for use in EVSE systems.

*Fixed and active power regulated schemes* (table 2 a) and b)) are used for the dominant distributed power generation connected to LV-networks, photovoltaic inverter systems. As solar radiation for one LV-network is nearly identical, networks

Table 2: Reactive power control by power factor  $\cos(\varphi)$  schemes:

Power Factor Scheme	a)	b)	c)
Power converter type	Fixed $\cos(\varphi)$	Active power regulated $\cos(\varphi(P))$	Voltage amplitude regulated $\cos(\varphi(U))$
Distributed renewable energy inverter [8]			
Adaption for high-power EVSE rectifiers			

voltage levels are highly correlated to photovoltaic infeed power. Providing inductive reactive power based on the instantaneous active power infeed, voltage rise is successfully reduced to ensure voltage quality. In LV-networks with DRE and EVSE systems, this control scheme suffers the problem of contrary goals. DRE systems provide inductive, EVSE capacitive reactive power, resulting in a partial compensation as shown in figure 7a).

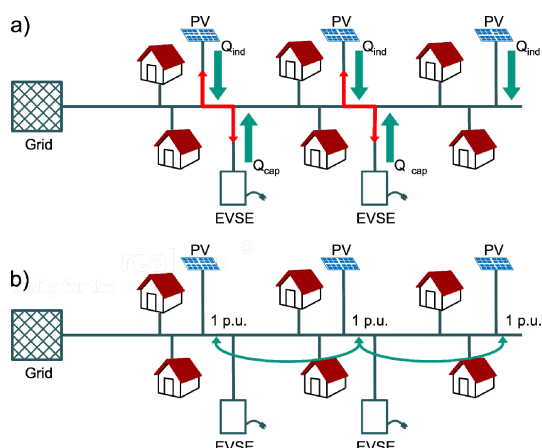


Figure 7: Power converter interactions

- Partial compensation of fixed and active power regulated  $\cos(\varphi)$
- Possible system instability of voltage amplitude regulated  $\cos(\varphi)$

The problem of partial compensation could be overcome by a *voltage amplitude regulated power factor scheme* (table 2 c)). The power factor defined is in uniform manner for each power converter. As network voltage varies over the cable length (as shown in section 3.1.2), each power converter operates at an individual set point controlled by its PCC voltage. Recognizing

that every power converter system has its own unique transient behavior, defined by semiconductor switching speed, electrical components dimensioning and control method and parameters, concerns about instability due to power converter interaction have been raised [9].

As the dynamic behavior of the scheme is not well defined, prior to rolling out this reactive power scheme in large scale, an experimental study [10] was conducted. A recommendation of a dead-time of 5 s in the reactive power control scheme was one of the key findings, preventing possible instability between multiple power converters. With this restriction in time response behavior, enhancement of voltage stability is limited to supply voltage stability (section 2.3.3). The potential of fast reactive power support to rapid voltage changes (section 2.3.2) requires control algorithms with enhanced dynamic behavior. The *voltage-droop control* approach is a suitable control method for providing high dynamic voltage support.

### 3.2.2 Voltage-Droop Control

In general, droop-control schemes are chosen for independent operating systems sharing the same optimization goal. This is achieved by weighting each systems' contribution to the overall regulation of the system with a droop factor. Considering the actual reactive power output of each involved power system by generating a droop between command variable signal  $U_{ref}$  and manipulated variable  $Q_{ref}$ , an individual set point  $U_{ref}^*$  is computed for each system (figure 8a). The value of  $m_{sloop}$  defines the sloop characteristic as shown in figure 8b.

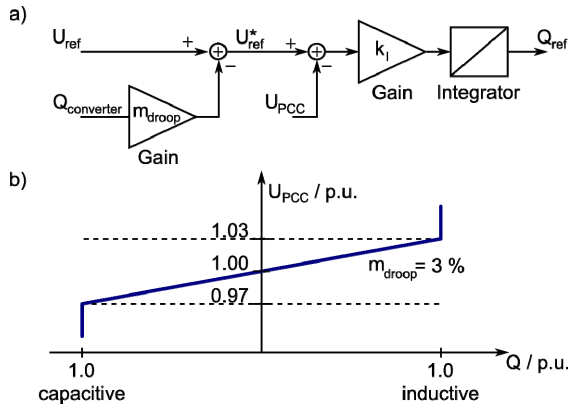


Figure 8: Voltage-droop control of reactive power

a) Block diagram of control structure

b) Reactive power output characteristics ( $m_{droop} = 3\%$ )

The integrator gain  $kI_Q$  adjusts the dynamic behavior of the system. Analytical approaches [11] to determine appropriate integrator gain parameters are based on several assumptions:

1. Voltage-droop controlled power converters are evenly distributed in the low-voltage system.
2. The nominal values of each system are identical.
3. The analytical approach neglects power converters dynamic response behavior.

In reality, nominal parameters and dynamic behavior of power converter differ depending on the application. Also, the line length between the power converters varies in a wide range. These differences are crucial for the stability of a voltage-droop control concept.

Table 3: Power converter parameter range

Parameter	Value	Unit	Description
$U_{Grid}$	400	V	Nominal voltage
$f_N$	50	Hz	Power frequency
$U_{DC}$	700	V	DC link nominal voltage
$S$	3 ... 200	kVA	Rated power
IGBT switching frequency			
$f_{IGBT}$	20	kHz	$S < 8$ kVA
	10	kHz	$8$ kVA $< S < 15$ kVA
	8	kHz	$15$ kVA $< S < 30$ kVA
	5	kHz	$30$ kVA $< S < 50$ kVA
	3	kHz	$S > 50$ kVA

## 4 Stability Study of Voltage-droop Reactive Power Control

### 4.1 Voltage Orientated Control Model for a Grid-tied Power Converter

Before we can determine the voltage-droop control parameters, a dynamic model for a grid-tied power converter is required. Therefore, the dimensioning of components, the transfer function of current and voltage control and the control loop design has to be done for each power converter. Each power converter is defined by its nominal power, semiconductor switching frequency, PCC voltage and DC-link voltage. The variation in these power converter is shown in table 3. The power converters' dynamics are derived from these parameters in three steps (figure 9).

1. Power converter components are dimensioned.
2. Calculation of the current and voltage transfer functions.
3. Parametrization of control parameters.

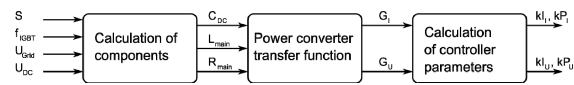


Figure 9: Calculation of power converter parameters

In the first step, *power converter components* are dimensioned. A frequently used calculation formula for the DC-link capacitance is

$$C_{DC} = \frac{S}{2 \cdot \pi \cdot f_N \cdot U_{DC} \cdot \Delta U_{DC}}, \quad (10)$$

where the DC-link voltage ripple  $\Delta U_{DC}$  is set to 10% of  $U_{DC}$ . The main inductance  $L_{main}$  value is estimated with respect to the IGBT switching frequency  $f_{IGBT}$  and a current ripple  $\Delta I_L$  of 6% of the power converters rated current  $I$ .

$$L_{main} = \frac{U_{Grid}}{8 \cdot \Delta I \cdot f_{IGBT}} \quad (11)$$

Derived by various resistance measurements of main inductance, the resistance  $R_{main}$  is approximated to

$$R_{main} = \frac{285 \cdot 10^{-6} \cdot S}{I^2}. \quad (12)$$

The *transfer function* is derived from system theory for voltage orientated control of grid-tied power converters (figure 10).

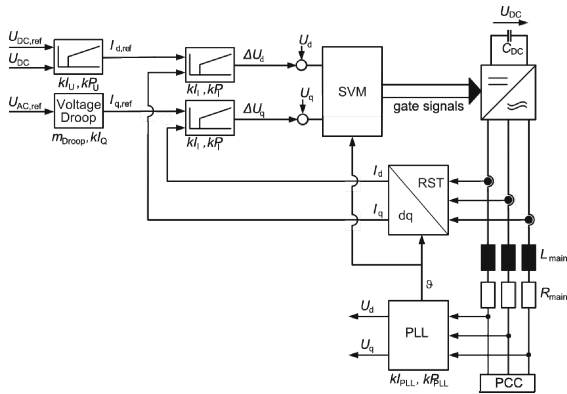


Figure 10: Control concept for grid-tied power converter

The *transfer function* for current control is given in (13).

$$G_I(s) = \frac{1}{R_{main} + sL_{main}} \cdot \frac{1}{1 + s \frac{1}{f_{IGBT}}} \quad (13)$$

The transfer function for DC-link voltage control is described by

$$G_U(s) = \sqrt{\frac{3}{2}} \cdot U_{Grid} \cdot \left( 1 - \frac{\frac{2}{3} \cdot sL_{main} \cdot S}{\left( \sqrt{\frac{3}{2}} \cdot U_{Grid} \right)^2} \right) \cdot \frac{1}{(1 + sT_i) \cdot (sC_{DC} \cdot U_{DC})} \quad (14)$$

where the current control deadtime is approximated by  $T_i = \frac{1}{\omega_{c,i}}$ .

Using MATLABs control system toolbox, the *control parameters* for current and voltage control are calculated for the highest controller bandwidth  $\omega_c$ , which still provides a phase margin of  $60^\circ$  for stable operation.

## 4.2 Simulative Voltage-droop Control Parametrization

### 4.2.1 Required Step-Response Behavior

For the determination of appropriate  $kI_Q$  parameters, two criteria are defined. The *overshoot* of reactive power output due to a sudden voltage sag or swell must be lower than 10 % (figure 11a). Inspired from consumer electronics voltage hold-on time [12], the *minimal response time* is set to 16 ms until 90 % of reactive power level is reached (figure 11b).

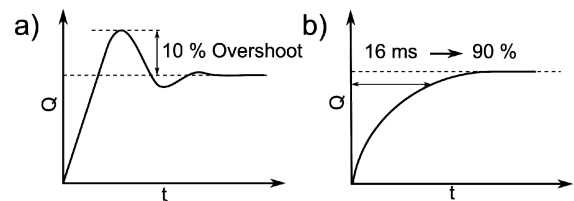


Figure 11: Step response design criteria for voltage-droop controlled reactive power output

### 4.2.2 Parametrization of Integral Gain

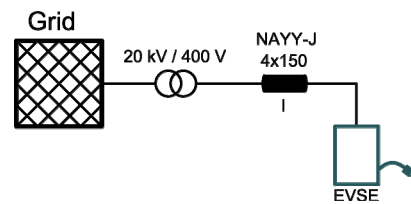


Figure 12: Simplified LV-network

A simplified LV-network connecting an EVSE via a cable (figure 12) to a local substation is used for  $kI_Q$  determination. The network parameters are selected according to table 1, using a cable length of 300 m. A rapid voltage sag and swell of 3 % and 30 % with a duration of 100 ms is applied as test stimulus (figure 13). The droop factor of the control scheme is set to  $m_{droop} = 3 \%$ .

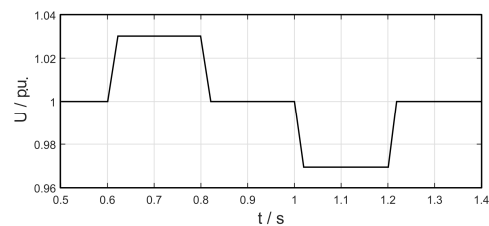


Figure 13: Voltage test stimulus with 3 % amplitude

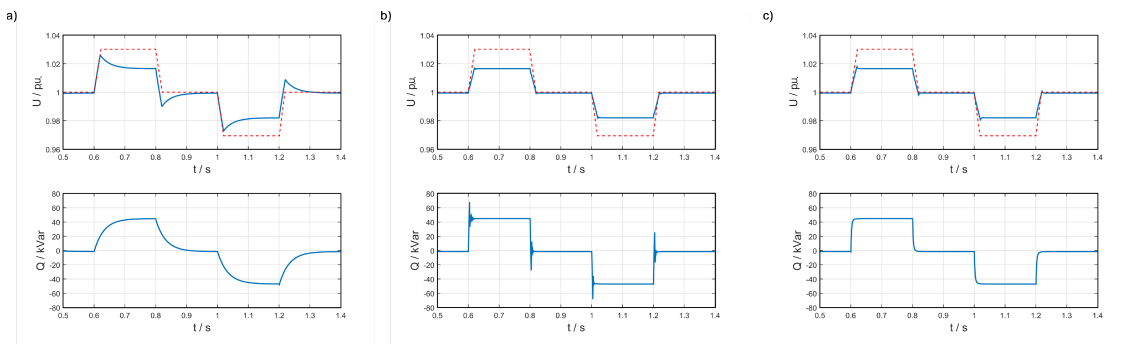


Figure 14: Evaluation method used for parametrization of voltage-droop controller  
 a) Minimum response time to slow    b) Reactive power overshoot exceeding 10 %    c) Both criteria fulfilled

A parameter sweep of the integral gain  $kI_Q$  has been simulated, until the required step-response behaviour was met with a tolerance of 1 %<sub>abs.</sub>. The parameter sweep was evaluated using the defined step-response criteria (figure 14) and for converter power ratings between 10 kVA and 200 kVA with a step size of 10 kVA. The results of this simulative parametrization are shown in figure 15.

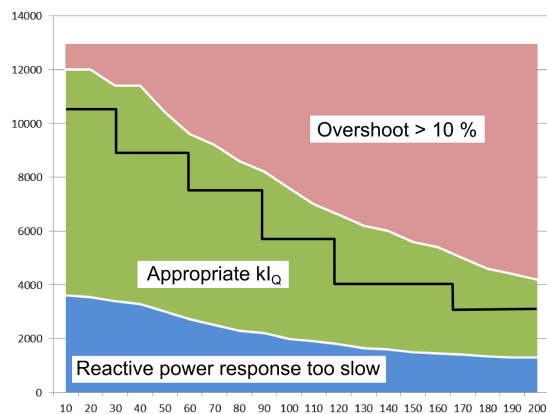


Figure 15: Reactive power step response  
 Red area: Overshoot criterium not met  
 Blue area: Minimal response longer than 20 ms  
 Green area: Both criteria fulfilled  
 Black curve: Selected parameter for further simulations

### 4.2.3 Probabilistic Parameter Verification Using Multiple Voltage-droop Controlled Power Converters

A typical German suburban LV-network is evaluated for probabilistic verification of stable voltage-droop control operation. A local substation feeds five parallel radial feeders (figure 16). Each feeder supplies six loads, with a distance of  $l = 50$  m between each load. The networks' parameters are according to table 1.

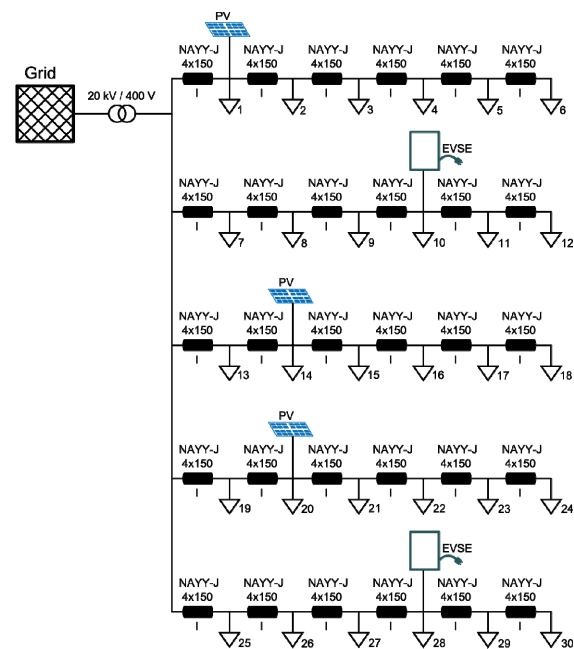


Figure 16: Example network scenario used for probabilistic verification:  
 PV inverter: PCC 1 (4 kVA), 14 (17 kVA), 20 (5 kVA)  
 EVSE rectifier: PCC 10 (67 kVA), 28 (27 kVA)

A total connection power of 120 kVA – equal to 33 % of local substations power – is split by random in a number of 4 to 6 power converters. For each power converter a random PCC is chosen, and its reactive power integral gain  $kI_Q$  has been selected as shown in figure 15. The test stimulus (figure 13) is applied to the grid voltage, and the reactive power response is analysed using the criteria defined in section 4.2.1.

For three different load scenarios (base load, mid load, peak load), a total number of 600 simulations were evaluated. In all cases, the step response criteria of the voltage-droop controller was met, proving the concept of voltage-droop control for mitigating supply voltage variation and rapid voltage changes.

## 5 Conclusion

Rules for grid connection of EVSE systems have been analyzed. Long line lengths between the local substation and an EVSE system can restrict grid access due to voltage stability issues. EVSE equipped with active rectifiers allow reactive power voltage support, which simplifies grid access. The interaction between DRE and EVSE power converters using power factor based compensation schemes are discussed, and the voltage-amplitude regulated power factor control is identified as suitable for voltage stability control.

Additional, the voltage-droop control of reactive power is analyzed for enhancing power quality by mitigating rapid voltage changes. Mass simulation is used for parametrization of the voltage-droop controller, and a probabilistic simulation with multiple voltage-droop controlled converters verifies the control concept.

## 6 Acknowledgments

This work was supported under a grant of the German Federal Ministry of Economics and Technology (BMWi) within the CROME project (Cross Border Mobility for Electric Vehicles; www.crome.eu) [Grant 01ME12002].

## References

- [1] National Platform for Electric Mobility (NPE), 2014, *4<sup>th</sup> Progress Report*, Joint Agency for Electric Mobility of the Federal Government (GGEMO), Berlin.
- [2] Standard *DIN EN 50160:2010 + Cor.:2010 Voltage characteristics of electricity supplied by public distribution networks*.
- [3] Bundesverband der Energie- und Wasserwirtschaft e.V., 2011, *TAB 2007 Technical conditions for connection to the low voltage network*, Edition 2011.
- [4] Standard *DIN EN-61000-3-11:2001-04 Electromagnetic compatibility (EMC): Limits; Limitation of voltage changes, voltage fluctuations and flicker in public low-voltage supply systems; Equipment with rated current  $\leq 75$  A and subject to conditional connection*.
- [5] Standard *DIN EN 61000-3-12:2012-06 Electromagnetic compatibility (EMC): Limits - Limits for harmonic currents produced by equipment connected to public low-voltage systems with input current  $> 16$  A and  $\leq 75$  A per phase*.
- [6] D-A-CH-CZ working group EMC, 2007, *D-A-CH-CZ Technical rules for the assessment of network disturbances*, 2<sup>nd</sup> Edition.
- [7] G. Kerber, 2011, *Capacity of Low Voltage Distribution Networks Due to Power generation of Small Photovoltaic Power Plants*, University Library Ludwig-Maximilians-Universität München, München, Germany.
- [8] VDE Application Rule, 2011, *VDE AR-N 4105 Generators connected to the low-voltage distribution network*.
- [9] T. Schaub, T. Meyer, J. Backes, E. Wieben, *Entwicklung und Untersuchung von Solarwechselrichtern mit spannungsabhängiger Blindleistungseinspeisung in Labor und Feld*, 25. Symposium Photovoltaik, Bad Staffelstein, 2010.
- [10] P. Esslinger, R. Witzmann, *Experimental study on voltage dependent reactive power control  $Q(V)$  by solar inverters in low-voltage networks*, E-ISBN 978-1-84919-732-8, 22nd International Conference and Exhibition on Electricity Distribution (CIRED 2013), Stockholm, 2013.
- [11] L. B. Perera, G. Ledwich, A. Ghosh, *Multiple distribution static synchronous compensators for distribution feeder voltage support*, IET Generation, Transmission & Distribution, Volume 6, Issue 4 (2012), ISSN 1751-8687, 285-293.
- [12] Intel Cooperation, *Power Supply -Design Guide for Desktop Platform Form Factors*, Revision 1.2, 2008.



**Peter Krasselt** received the diploma in electrical engineering from the Karlsruhe Institute of Technology, Karlsruhe, Germany, in 2010, where he is currently working towards the Ph.D. degree. His research interests include modeling, simulation and experimental analysis of optimized grid integration for high-power DC charging infrastructures.



**Jonas Boßle** received the B.Sc. and M.Sc. degree in electrical engineering from the Karlsruhe Institute of Technology, Karlsruhe, Germany, in 2012 and 2015, respectively. His research interests include modeling and control of power electronics.



**Michael R. Suriyah** received his PhD in electrical engineering from the Karlsruhe Institute of Technology, Karlsruhe, Germany, in 2013. Today he is leading the division on power networks at the KIT.



**Thomas Leibfried** (M'96) was born in Neckarsulm, Germany, in 1964. He received the Dipl.-Ing. and Dr.-Ing. degrees in electrical engineering from the University of Stuttgart, Stuttgart, Germany, in 1990 and 1996, respectively. From 1996 to 2002, he was with the Siemens AG, Nuremberg, working in the power transformer business in various technical and management positions. In 2002, he joined the University of Karlsruhe (now Karlsruhe Institute of Technology, KIT) as Head of the Institute of Electric Energy Systems and High-Voltage Technology. He is the author of more than 70 technical papers. Prof. Leibfried is a member of Verband der Elektrotechnik Elektronik Informationstechnik and CIGRE.